

A Study on Thermal Conductivity and Stability of Nanofluids Containing Chemically Synthesized Nanoparticles for Advanced Thermal Applications

Sujoy Das, Krishnan Bandyopadhyay, and M.M. Ghosh

(Submitted August 1, 2017; in revised form May 7, 2018; published online July 12, 2018)

This study presents easy methods of synthesizing silver (Ag) and copper (Cu) nanoparticles through chemical route in an aqueous medium under atmospheric condition at ambient temperature. The synthesized nanoparticles have been characterized with different techniques, such as x-ray diffraction, Fourier transform infrared spectroscopy, field emission scanning electron microscopy, energy-dispersive x-ray spectroscopy, high-resolution transmission electron microscopy, UV–visible spectroscopy and dynamic light scattering measurements. Experimental observations have revealed the absence of any metal oxide layer around the nanoparticles which are found to remain stable under ambient conditions. The featured properties, such as narrow size distribution, stability, make these nanoparticles potential candidates for the synthesis of effective nanofluids. The nanofluids have been prepared by dispersing the nanoparticles synthesized through chemical route in a suitable base fluid. The thermal conductivity of nanofluids with different nanoparticles loading has been measured by transient hot-wire method, and the results have shown that the increasing trend of enhancement in thermal conductivity with respect to nanoparticles concentration is attainable only when the nanoparticles concentration is below some limiting value depending on the type of nanofluid. Beyond this limiting value of loading, the thermal conductivity of the nanofluid decreases due to pronounced agglomeration effect. The measurements of thermal conductivity of nanofluids over varying temperatures for a given volume fraction loading of nanoparticles have shown that the thermal conductivity increases markedly with the increase in temperature. Hence, nanofluids are likely to be much more promising at high-temperature applications.

Keywords Ag nanoparticles, Cu nanoparticles, nanofluid, stability, thermal conductivity

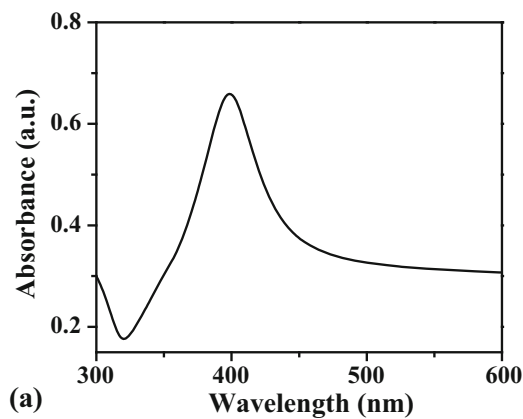
1. Introduction

Nanofluids are attracting increasing interest due to their high potential applications in transportation, microelectronics, aerospace, medical and manufacturing sectors. The low thermal conductivity (k) of common heat transfer fluids, such as water, ethylene glycol (EG), propylene glycol, engine oil, results in poor heat transfer performance of these fluids and, thus, is a serious limitation in improving the performance and compactness of engineering equipments, particularly miniaturized electronic devices, which need rapid rate of heat dissipation. Research and development activities were undertaken to improve the heat transport properties, especially the thermal conductivity and convective heat transfer coefficient of the coolant fluids. It is found that the thermal conductivity of metallic (e.g., Ag, Au, Cu, Fe), metallic oxide (e.g., CuO, Al₂O₃, TiO₂) or non-metallic materials, such as carbon nanotube, is some order of magnitude higher than the conventional heat transfer fluids. It is, thus, an innovative idea trying to enhance thermal conductivity by adding solid particles

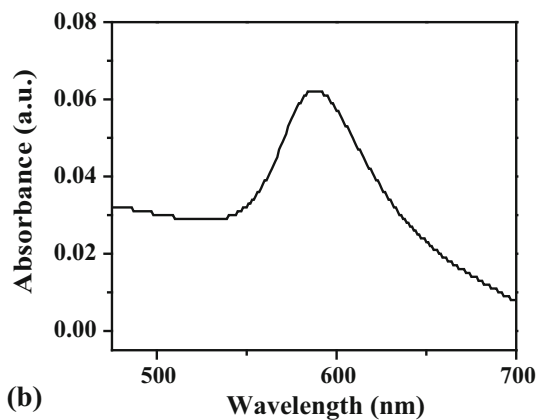
into conventional heat transfer fluids in order to change heat transfer nature of the fluids (Ref 1). At the very beginning of this kind of attempt, solid particles of micrometer and/or millimeter sizes were blended into the base fluids to make suspensions or slurries. However, large solid particles cause several problems, such as rapid settling of these particles, abrasion and erosion of the surface of the channels through which the fluid flows, clogging of the microchannels, increasing the pressure drop, a low stability of the fluids, which substantially limit the practical applications (Ref 2, 3). The situation has changed when researchers have tried to suspend various metal and metal oxide nanoparticles in various heat transfer fluids and obtained promising results (Ref 4–6). However, many things remain elusive about these suspensions of nanostructured materials, in particular, the mechanism of heat transfer through these fluids. Choi coined the name ‘nanofluid’ to this newly developed highly efficient heat transfer fluid, containing nanosized particles of various materials.

To investigate the above concept, colloidal dispersion of nanometer-sized particles in common heat transfer fluids, popularly known as ‘nanofluids,’ has been attempted by many researchers (Ref 5, 6). The interesting properties of nanoparticles, such as large surface area to volume ratio, dimension-dependent physical properties, high mobility, can be exploited in the nanofluids. At the same time, small size and low weight would make nanoparticles better and more stably dispersed in carrier fluids giving rise to high stability of nanofluids. As a result, nanofluids have attracted considerable research interest due to their enhanced thermal conductivities compared to their base fluids (Ref 7 and 8) and long-term stability than those of

Sujoy Das, Krishnan Bandyopadhyay, and M.M. Ghosh, Department of Metallurgical and Materials Engineering, National Institute of Technology, Durgapur, West Bengal 713209, India. Contact e-mail: mmgnitd@gmail.com.



(a)

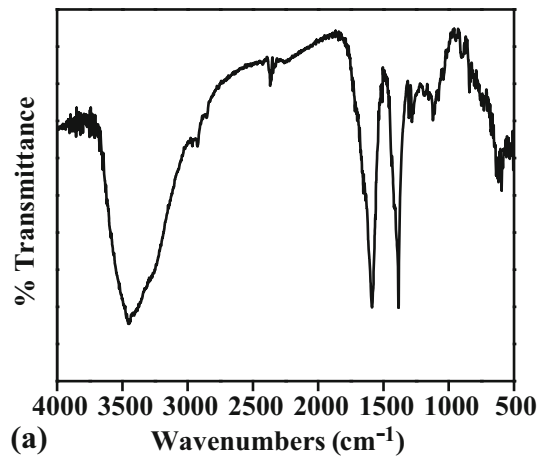


(b)

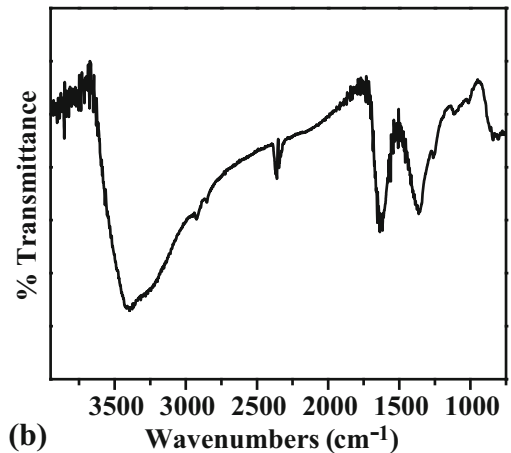
Fig. 1 UV-Vis absorption spectrum of (a) silver and (b) copper nanoparticles

the suspensions of millimeter or even micrometer-sized particles. Eastman et al. have reported a 40% enhancement in thermal conductivity of ethylene glycol by adding small volume percent of copper nanoparticles with a diameter smaller than 10 nm (Ref 6). The thermal conductivity enhancement of nanofluids was found to be dependent of temperature, and the increase in effective thermal conductivity of nanofluids with increasing temperature makes them promising for applications at elevated temperatures (Ref 9). Another interesting phenomenon of nanofluids is that even extremely low concentration of nanoparticles dramatically increases the critical heat flux in a pool boiling system (Ref 10). The low cost and high availability of copper whose thermal conductivity is near to silver make copper nanoparticle an attractive candidate for the preparation of nanofluids for industrial applications.

Our aim in the present contribution is to synthesize silver and copper nanoparticles through chemical route and then to prepare stable nanofluids by incorporating these nanoparticles into suitable base fluids. Herein, we report an aqueous phase synthesis route for pure silver and copper nanoparticles. The synthesis involves the reduction of silver(I) and copper(II) salts by a suitable reducing agent in the presence of a capping agent without any inert gas protection. The morphologies and structures of the nanoparticles were characterized by field emission scanning electron microscopy (FESEM), high-resolution transmission electron microscopy (HRTEM), UV-visible spectroscopy (UV-Vis), Fourier transform infrared (FTIR) spectroscopy, powder x-ray diffraction (XRD) and dynamic light scattering (DLS) experiments. In the two-step process of



(a)



(b)

Fig. 2 FTIR spectrum of coated (a) silver and (b) copper nanoparticles

nanofluid synthesis, the nanoparticles produced through chemical route are dispersed uniformly in the base fluid to produce highly effective and stable nanofluids. The effective thermal conductivity of silver and copper nanofluids was measured as a function of volume fraction loading of nanoparticles by transient hot-wire (THW) method. In addition, we have investigated the effect of agglomeration on the thermal conductivity of nanofluids.

2. Experimental

All the chemicals used in our experiments were of analytical grade and were used without further purification.

2.1 Synthesis of Silver Nanoparticles

Solution of silver nitrate was prepared by dissolving 5 g of AgNO_3 in 50 mL deionized water in a 500-mL three-neck flask. To this solution, 150 mL of 0.7 M trisodium citrate was added dropwise under magnetic stirring at room temperature. After complete addition of trisodium citrate, magnetic stirring was continued for about half an hour. Then, aqueous solution of sodium formaldehyde sulfoxylate (0.85 M, 50 mL) was added slowly to obtain dark gray precipitate. The precipitated particles

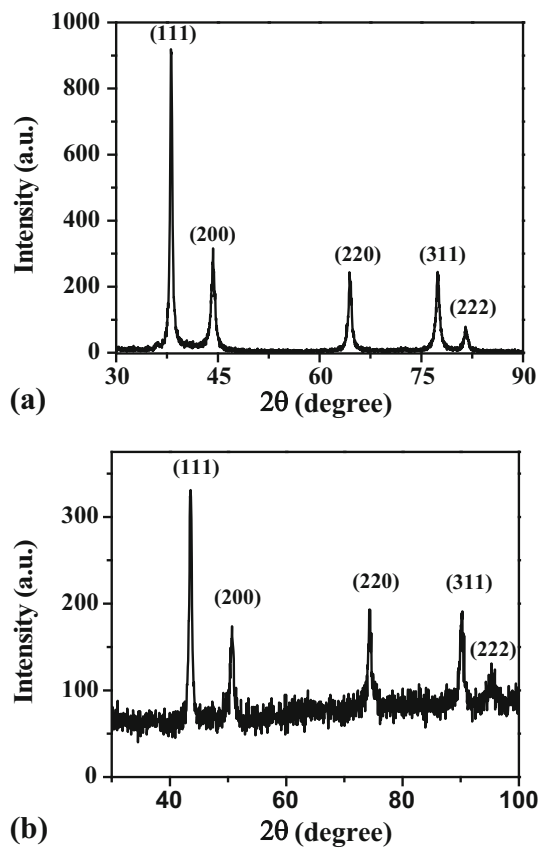


Fig. 3 XRD pattern of (a) silver and (b) copper nanoparticles

were separated by filtering, washed several times with methanol and then dried.

2.2 Synthesis of Copper Nanoparticles

In the present work, wet chemical reduction method is used to synthesize copper nanoparticles in the presence of water as solvent under ambient atmosphere. An appropriate amount of cetyl trimethyl ammonium bromide (CTAB) (0.02 M) was dissolved in deionized water to obtain a transparent solution. Then, 0.04 M of cupric chloride was added to the aqueous solution of CTAB under magnetic stirring for 30 min at room temperature. The pH of the solution was maintained at 10. Finally, excess hydrazine hydrate (0.5 M), which acts as a reducing agent, was added slowly to the above solution under constant stirring. The resulting solution was left for stirring for another few hours to allow complete particle growth. The solution turned brown in color confirming the formation of copper nanoparticles. The particles were separated by filtering, washed several times with ethanol and then dried under vacuum.

2.3 Preparation of Nanofluids

To prepare silver nanofluids of different volume concentrations, the calculated mass of the silver nanoparticles was dispersed in deionized water under intensive and prolonged ultrasonication. Copper nanofluids of different volume concentrations were obtained by dispersing an appropriate amount of dried copper nanoparticles in ethylene glycol under ultrasonic vibration. To get a uniform dispersion and stable suspension,

the nanofluids were kept under ultrasonic vibration continuously for few hours.

2.4 Characterization

After synthesis, the samples were characterized by different techniques. The x-ray diffraction (XRD) patterns of the samples were recorded using the Cu K α radiation ($\lambda = 0.15406$ nm) in a x-ray diffractometer (X'Pert PRO, PANalytical BV, PW3040/60, the Netherlands) at a scanning rate of 0.02° per step in the 2θ range from 20° to 110° . Fourier transform infrared (FTIR) spectra were recorded with a Fourier transform infrared spectrophotometer (Nicolet 6700) within the range from 4000 to 400 cm^{-1} wave numbers. Synthesized samples were studied by UV-Vis absorption spectroscopy from a double-beam spectrophotometer (Varian Carry 100). The morphologies and compositions of the nanoparticles were examined by field emission scanning electron microscope (FESEM) (model: JSM-6700F, JEOL, Japan) equipped with an energy-dispersive x-ray spectrometer (EDX). High-resolution transmission electron microscopic (HRTEM) observations were carried out using JEOL 2100 electron microscope at 200 kV accelerating voltage. The particle size distribution and hydrodynamic radii were analyzed by dynamic light scattering (DLS) measurement technique using Nano-Zetasizer ZS (Malvern Instruments, UK). The transient hot-wire (THW) method was employed for measuring thermal conductivity of nanofluids using KD2 Pro thermal property analyzer (Decagon devices, Inc.).

3. Results and Discussion

3.1 UV-Visible Spectroscopic Analysis

UV-visible spectroscopy is one of the most widely used techniques for structural characterization of metal nanoparticles. In Fig. 1(a), we present the UV-visible spectrum of the silver nanoparticles in solution. The absorption spectrum consists of a single sharp surface plasmon resonance (SPR) band at ≈ 399 nm, indicating the presence of spherical silver nanoparticles (Ref 11). In Fig. 1(b), we present the UV-visible absorption spectrum of the copper nanoparticles in aqueous solution. The characteristic absorption peak at around 587 nm can be attributed to the excitation of surface plasmon resonance of copper nanoparticles (Ref 12). The peak position of the synthesized copper nanoparticles is little bit red shifted about 10 nm as compared with the reported value (≈ 577 nm) (Ref 13). The small red shift in the peak position of the copper nanoparticles is indicating that the peak position depends not only on the size and shape but also on the capping agent (Ref 14). In addition, the absence of absorption maximum at 800 nm is implying the formation of non-oxidized copper nanoparticles (Ref 13). This revealed that the complete reduction of copper ions into copper nanoparticles with narrow size distribution would be possible with this approach.

3.2 Characterization of Surface Coating Layer

FTIR spectroscopy is a useful technique for characterizing the organic molecules present in the coating layer of the nanoparticles. Figure 2(a) shows the FTIR spectrum of citrate-stabilized silver nanoparticles. As compared to the FTIR spectrum of trisodium citrate (Ref 15), we observed the

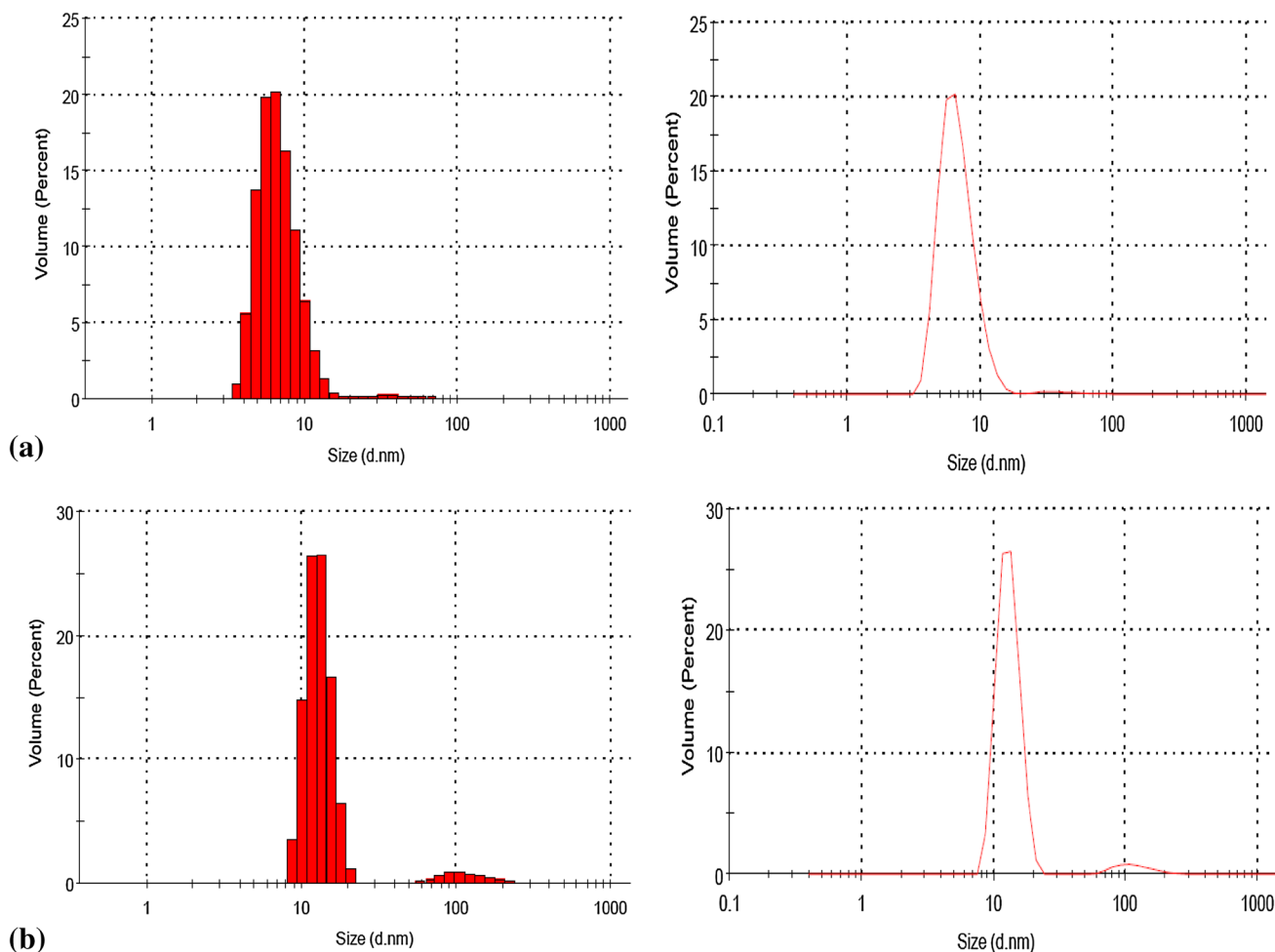


Fig. 4 Size distribution of (a) silver nanoparticles dispersed in water and (b) copper nanoparticles dispersed in ethylene glycol

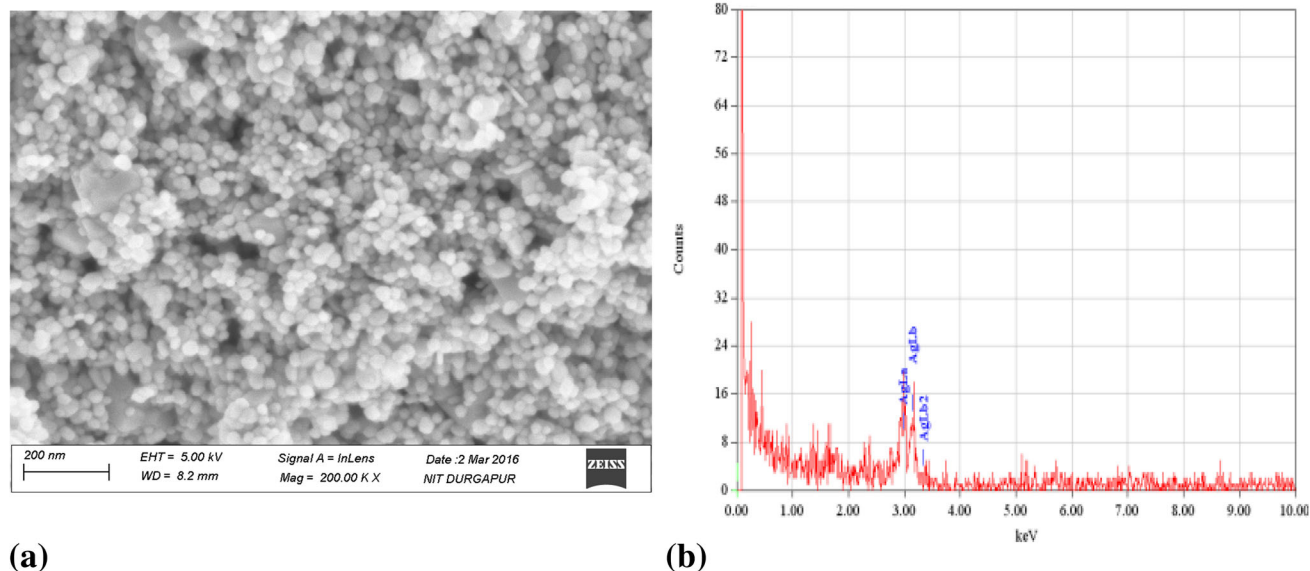
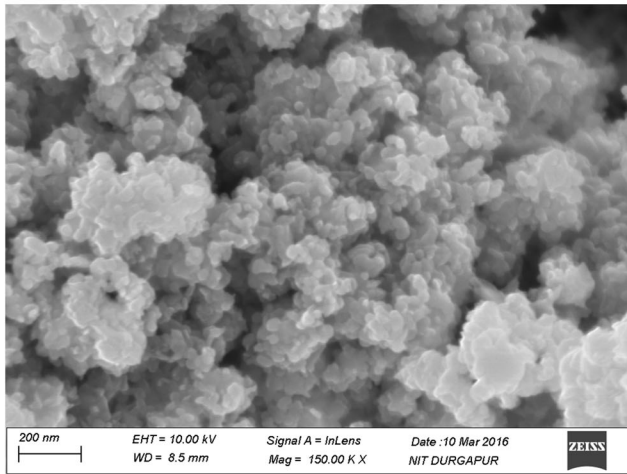


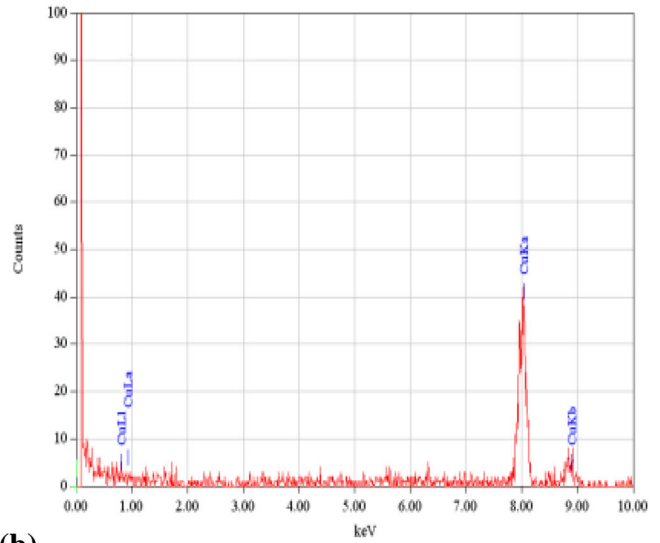
Fig. 5 The (a) SEM image and (b) EDX pattern of silver nanoparticles

presence of characteristic bands of trisodium citrate in the synthesized silver nanoparticles. For instance, the symmetric stretching of COO^- at 1394 cm^{-1} shifted to 1389 cm^{-1} and

asymmetric stretching of COO^- at 1589 cm^{-1} shifted to 1584 cm^{-1} . The broad peak at 3454 cm^{-1} is assigned to be OH stretching vibrations from adsorbed moisture. Figure 2(b)



(a)



(b)

Fig. 6 The (a) SEM image and (b) EDX pattern of copper nanoparticles

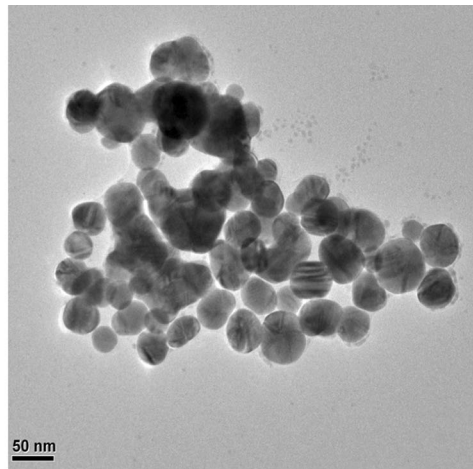
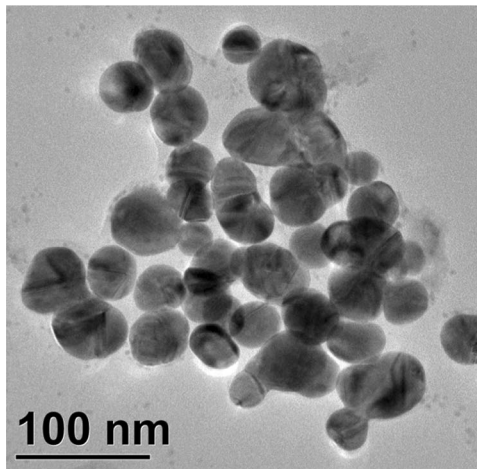
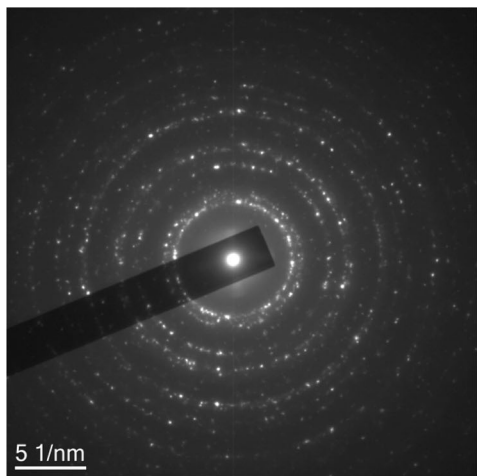
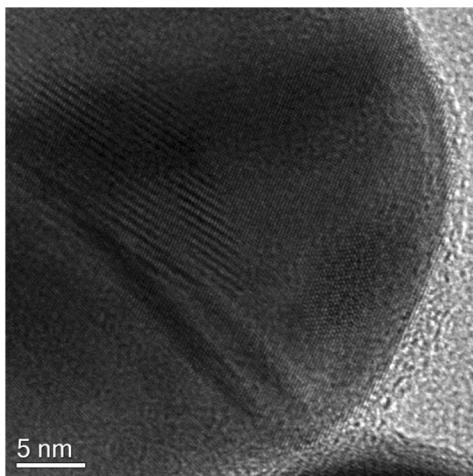


Fig. 7 TEM images of silver nanoparticles



(a)



(b)

Fig. 8 (a) SAED pattern and (b) lattice fringes obtained from HRTEM testing of silver nanoparticles

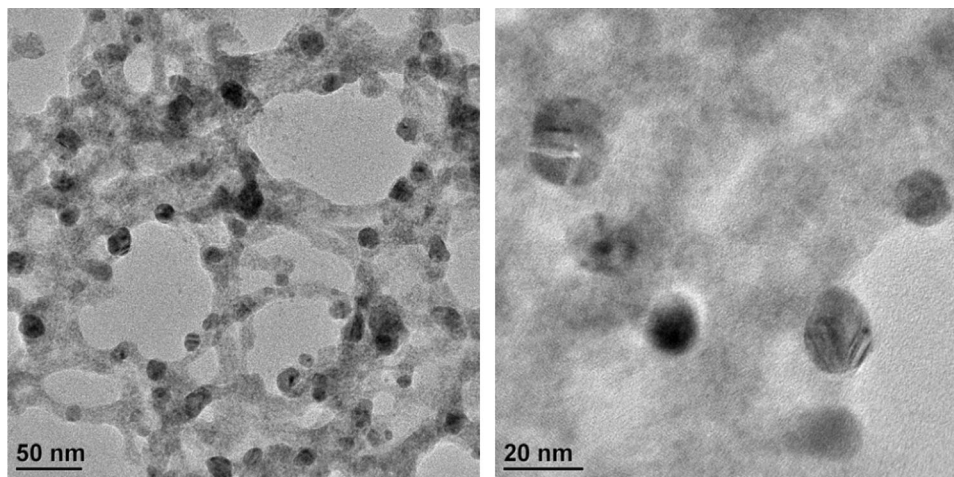


Fig. 9 TEM images of copper nanoparticles

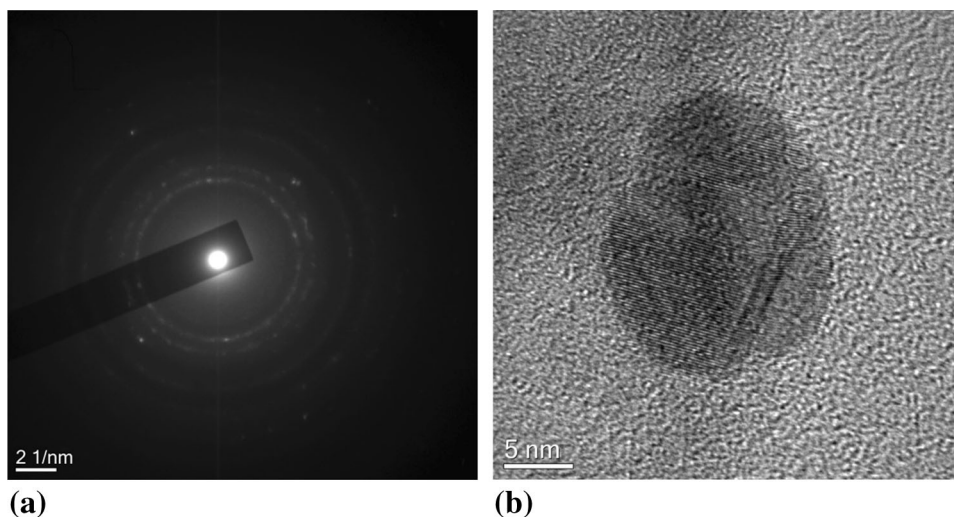


Fig. 10 (a) SAED pattern and (b) lattice fringes obtained from HRTEM testing of copper nanoparticles

shows the FTIR spectra of CTAB-stabilized copper nanoparticles. For the synthesis of copper nanoparticles in the presence of CTAB, there is always a small amount of CTAB adsorbed on the surface of the copper nanoparticles, which could work as a stabilizer. Compared with the FTIR spectrum of pure CTAB (Ref 16), the two peaks corresponding to the CH_2 stretching vibrations are shifted to higher wave numbers (2925 and 2852 cm^{-1}) reflecting the surface coating characteristics of copper nanoparticles. The broad peak from 3500 to 3100 cm^{-1} is attributed to the OH stretching vibrations of CTAOH. The pH values play a significant role in the reduction of Cu^{2+} . Interestingly, when the solution pH was adjusted to basic (pH 10) condition, the formation of cetyl trimethylammonium hydroxide (CTAOH) is favored which sticks to the surface of copper nanoparticles (Ref 17). These results certified that the surface of synthesized nanoparticles is coated with the capping agent.

3.3 X-ray Diffraction Measurements

The XRD pattern of the as-synthesized silver nanoparticles is shown in Fig. 3(a). It can be found that the diffraction peaks

with strong intensities appear at 2θ values corresponding to (111), (200), (220), (311) and (222) planes of face-centered cubic (fcc) structure of silver. The average crystallite size of the silver nanoparticles was calculated to be 19.3 nm on the basis of full width of half maximum of the (111) diffraction peak using Debye–Scherrer formula (Ref 18). Figure 3(b) shows the XRD pattern of the synthesized copper nanoparticles. All the diffraction peaks of the XRD pattern have been indexed to that of fcc copper phase without any impurities such as copper oxides (CuO , Cu_2O). The diffraction peaks with strong intensities appear at angles corresponding to the (111), (200), (220), (311) and (222) planes of copper, respectively. The average crystallite size of the copper nanoparticles determined by Debye–Scherrer equation (Ref 18) on peak (111) was 15.3 nm .

3.4 Dynamic Light Scattering (DLS) Measurements

Dynamic light scattering (DLS) was used for measuring the hydrodynamic size distribution of the synthesized nanoparticles dispersed in liquid phase. Figure 4(a) and (b) shows the particle size distribution of the silver and copper nanoparticles,

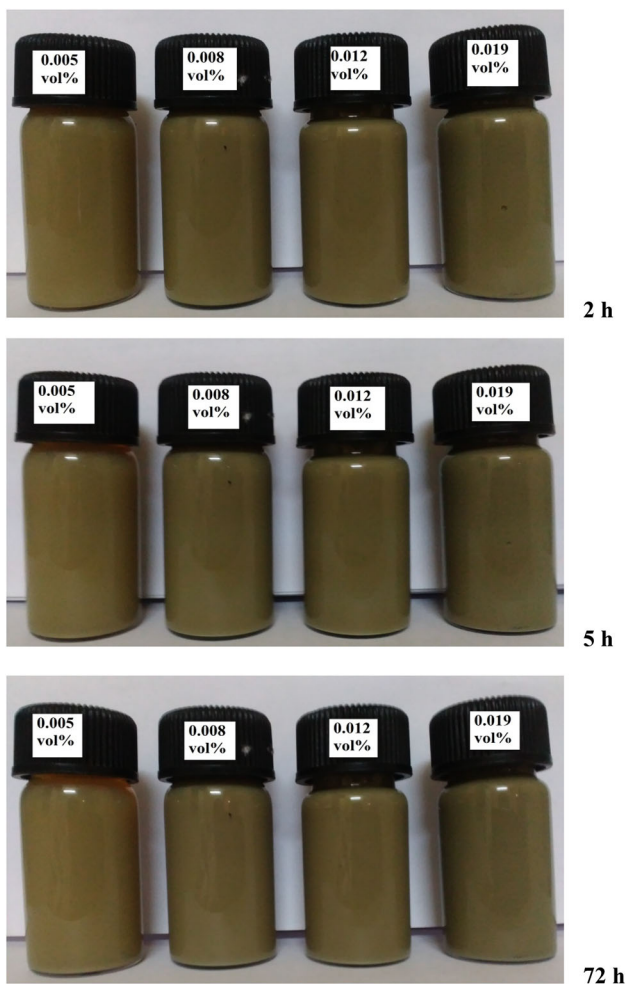


Fig. 11 Photographs of silver nanofluids with different volume fractions, at different instances of time after synthesis

respectively. After analyzing the data, it was found that the size of silver nanoparticles was in the range of 4–38 nm. The highest fraction of silver nanoparticles present in the solution was of 7 nm. Similarly, it was observed that the size of copper nanoparticles was in the range of 9–180 nm. However, beyond 25-nm range the percentage of nanoparticles present is very less. The maximum fraction of Cu nanoparticles present in the solution was of 16 nm. From the DLS measurements, it has been observed that the mean diameter of Ag and Cu nanoparticles is 7 nm and 16 nm, respectively, with a narrow size distribution (Fig. 4a and b).

3.5 Morphological Analyses

Field emission scanning electron microscopy (FESEM) was used to study the morphology of the synthesized silver and copper nanoparticles. Figure 5(a) and 6(a) show the FESEM images of the silver and copper nanoparticles, respectively. These show weakly agglomerated and roughly spherical particles with smaller size. The capping agent played a key role to prevent the tendency of agglomeration and coalescence of nanoparticles. The chemical composition and purity of the synthesized nanoparticles were examined using EDX analysis equipped on the FESEM. The EDX spectrum only exhibits the characteristics peaks of silver (Fig. 5b) and copper (Fig. 6b), suggesting that the synthesized nanoparticles are quite pure.

The TEM images of the silver nanoparticles are shown in Fig. 7. The TEM images reveal that the silver nanoparticles are spherical in shape with homogeneous distribution. The selected area diffraction pattern (SAED) (Fig. 8a) of the synthesized silver nanoparticles is characterized by five diffraction rings which correspond to (111), (200), (220), (311) and (222) planes, confirming the crystalline nature of the particles with fcc phase which have already confirmed by XRD analysis. The clear and uniform lattice fringes observed in the HRTEM presented in Fig. 8(b) indicate the high crystallinity of the silver nanoparticles. Figure 9 shows the TEM images of the as-prepared copper nanoparticles. The particles are spherical in shape and monodispersed, revealing that the presence of CTAB indeed restricted the growth of copper nanoparticles efficiently. The size of the copper nanoparticles observed in the TEM image is in the range of 12–16 nm, in good agreement with the result obtained from the XRD pattern. The diffraction rings revealed in Fig. 10(a) confirm the crystalline nature of fcc copper nanoparticles. In addition, the lattice fringes observed by close inspection with HRTEM (Fig. 10b) confirm highly crystalline nature of synthesized copper nanoparticles.

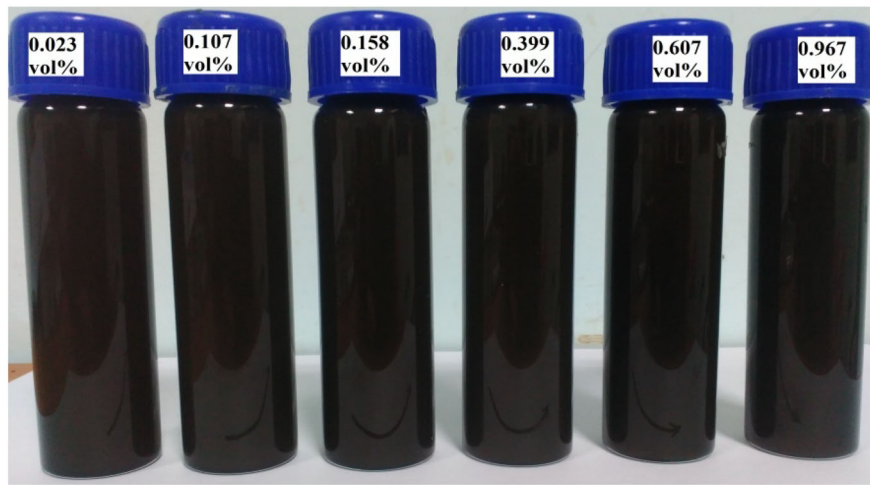
3.6 Stability Characteristics of Nanofluids

It is essential to investigate systematically the stability of nanofluids to exploit their practical applications. The stability of the synthesized nanofluids was assessed by visual examination of freshly prepared nanofluids with progress of time and to monitor any possible sedimentation with respect to time. The photographs taken at different instances after the synthesis of silver nanofluids (Fig. 11) with different volume fractions show that there is no observable particle sedimentation in any of the sample with respect to time and it is stable for 72 h studied presently. Figure 12 shows the photographs of copper nanofluid with different volume fractions at different time instances after synthesis. It reveals the sedimentation of copper nanoparticles for 0.607 and 0.967 initial vol.% at 72 h. The other volume fractions of copper nanofluids are quite stable up to 72 h. This result suggests that the copper nanofluids with high volume fractions possess weak stability as compared to nanofluids with low volume fractions.

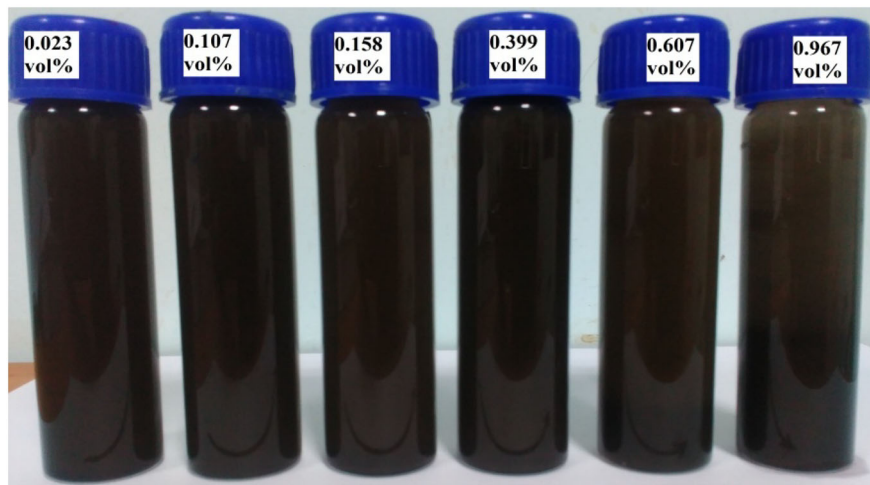
3.7 Thermal Conductivity Measurement

In the present research, we have devised an easy synthesis method of silver and copper nanoparticles through chemical route without any inert gas protection. This synthesis method employs an aqueous solution under atmospheric condition at room temperature. This approach is highly effective and also economical. The nanofluids have been prepared by dispersing the nanoparticles in a suitable base fluid without the addition of any external additive or dispersant. The thermal conductivities of water-based Ag-nanofluid and EG-based Cu-nanofluid have been measured with varying volume fraction loading of nanoparticles and temperature. The main focus of the present parametric type of study is to make a comparative assessment of the effectiveness of two types of nanofluids, viz. Ag- and Cu-nanofluids, prepared through the same route and come up with the most effective nanofluid.

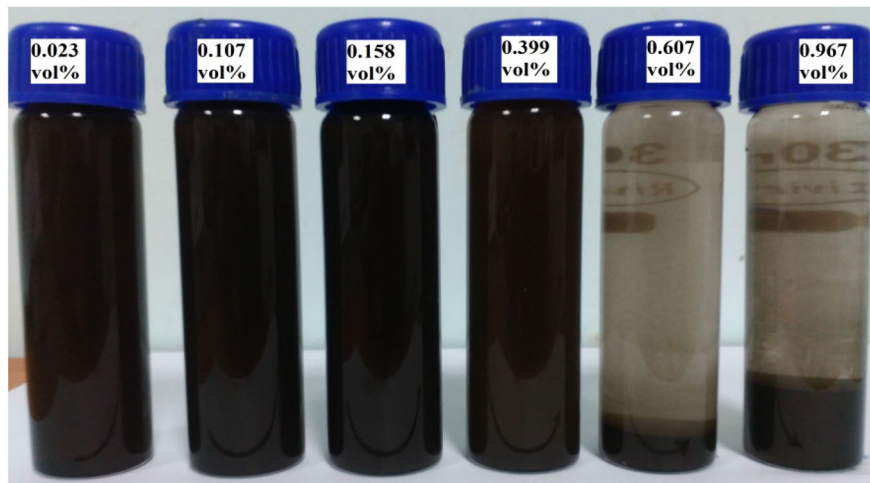
The effective thermal conductivity of nanofluids at room temperature as well as higher temperature was measured using transient hot-wire (THW) technique (Ref 19). Figure 13(a) shows the effective thermal conductivity as a function of volume fraction loading of silver nanoparticles in water-based



2 h



5 h



72 h

Fig. 12 Photographs of copper nanofluids with different volume fractions, at different instances of time after synthesis

Ag-nanofluid. It has been observed that the thermal conductivity of Ag-nanofluid increases in a nonlinear fashion with the increase in Ag nanoparticles loading. Several models have been proposed to account for the thermal conductivity enhancement of nanofluids, which include the Brownian motion of nanoparticles (Ref 20), liquid layering (Ref 21), ballistic transport (Ref 22) and the thermal conductivity difference between the

dispersed phase and the base fluid (Ref 23). In case of nanofluid, the thermal conductivity enhancement cannot be explained solely by just one mechanism. At higher volume fraction of Ag nanoparticles in the nanofluid, the interparticle distance between the particles becomes smaller which affects positively to the heat flow. It is clear that the larger the number of nanoparticles, the higher will be the thermal conductivity

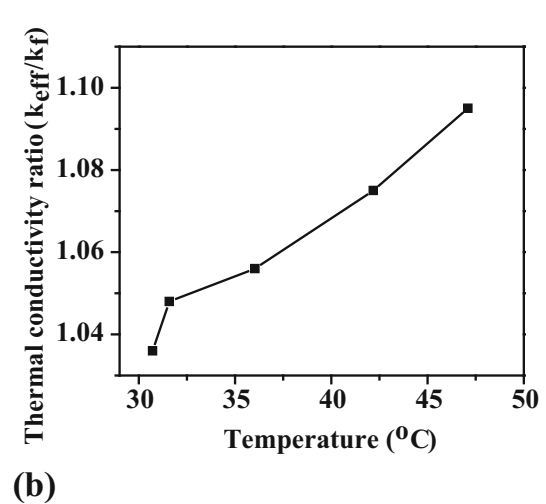
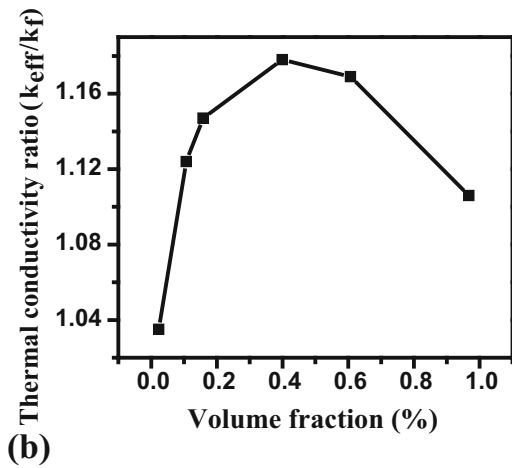
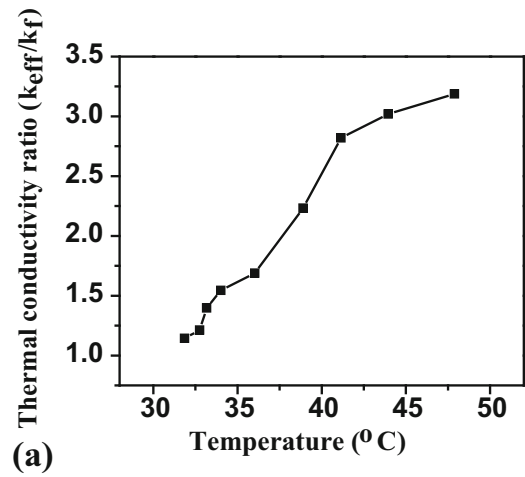
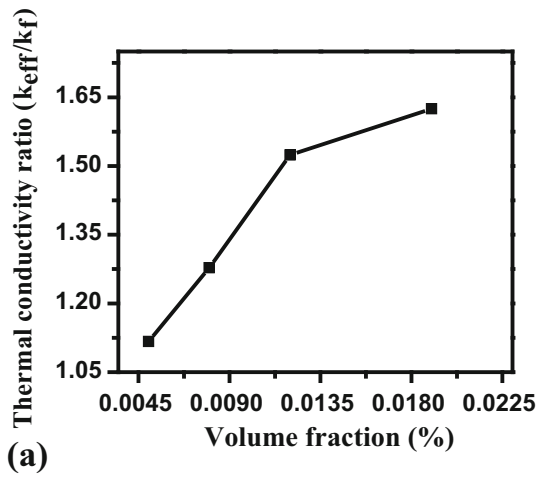


Fig. 13 Effective thermal conductivity of (a) silver nanofluid and (b) copper nanofluid, as a function of volume fraction loading

Fig. 14 Thermal conductivity ratio of (a) silver nanofluid and (b) copper nanofluid, as a function of temperature, for a given volume fraction loading

enhancement. This agrees with the Maxwell–Garnett model (Ref 24). Paul et al. reported 21% enhancement of thermal conductivity of silver nanofluid with average particle size of 55 nm at 0.1 vol.% loading (Ref 25). In the present work, the maximum enhancement of thermal conductivity of silver nanofluid is obtained as 62.5% at 0.02 vol.% loading. Figure 13(b) shows the effective thermal conductivity as a function of volume fraction of copper nanoparticles in ethylene glycol-based Cu-nanofluid. It has been observed that the thermal conductivity of Cu-nanofluid also increases initially in a nonlinear fashion with the increase in volume fraction (up to 0.399 vol.%) and, thereafter, decreases at still higher volume fraction, which contradict to the existing theoretical models. The maximum enhancement of thermal conductivity of copper nanofluid is obtained as 17.76% at 0.399 vol.% loading. In the present study, the thermal conductivity value was found to be lower than the corresponding value reported by Eastman et al. (Ref 6). The reason for the deterioration of thermal conductivity is due to the agglomeration of Cu nanoparticles with the increase in the volume fraction. Addition of more Cu nanoparticles in a fixed volume of carrier fluid (i.e., ethylene glycol) can be considered as congestion in particles movement in the nanofluid. At higher volume fraction, the Cu nanoparticles tend to agglomerate, which in turn reduces particle/fluid interfacial area. The agglomeration is likely to settle in the nanofluid due

to larger mass that results in particle gradient in the fluid (Ref 26). Some literature (Ref 27–29) also reported a decrease in thermal conductivity of nanofluid at higher volume fraction loading, due to appreciable particle agglomeration. The agglomeration of nanoparticles results in a decrease in the effective surface area to volume ratio. Therefore, the reduction of effective surface area of thermal interaction of nanoparticles results in a decrease in thermal conductivity of nanofluid. It is believed that the stability of a nanofluid is a vital factor for the effective thermal conductivity. Figure 12 evidences no significant amount of sedimentation up to 0.399 vol.% loading of copper in ethylene glycol-based nanofluid up to 72 h of holding under stagnant condition. But above 0.399 vol.% loading, the sedimentation was observed with progress of time and a gray precipitate was found at the bottom of the vial at 72 h. To improve the long-term stability of nanofluids, it is essential that the nanoparticles should be in well-dispersed form without any agglomeration and should be uniformly small size required for Brownian motion. At higher concentration, the presence of large number of nanoparticles per unit volume results in agglomeration, and hence, the effective thermal conductivity of the nanofluid decreases dramatically for the loading of Cu nanoparticles beyond 0.399 vol.% in ethylene glycol. At higher

Table 1 Comparison of typical thermal conductivity values of present nanofluids with those of the fluids conventionally used in industries for heat transfer purpose

Fluids	Conventional heat transfer fluids		Present nanofluids			
	Water	EG	Water-based Ag-nanofluid (at 0.02 vol.% loading and 25 °C temperature)	Water-based Ag-nanofluid (at 0.006 vol.% loading and 48 °C temperature)	EG-based Cu-nanofluid (at 0.399 vol.% loading and 25 °C temperature)	EG-based Cu-nanofluid (at 0.02 vol.% loading and 47 °C temperature)
Thermal conductivity, W m ⁻¹ K ⁻¹	0.59	0.25	1.001	1.94	0.305	0.276

particle concentration, the formation of agglomerates in the nanofluid facilitates due to Van der Waals forces of attraction. The agglomeration of nanoparticles is known to have negative impact on stability as well as the thermal conductivity of the nanofluid, and the agglomeration size increases with the loading of nanoparticles (Ref 30 and 31). Hence, loading of copper nanoparticles in ethylene glycol enhances the thermal conductivity up to a maximum value. Thereafter, the thermal conductivity decreases with further addition of copper nanoparticles, due to the agglomeration effect.

Figure 14 shows the thermal conductivity ratio of the Ag (0.006 vol.% loading)- and Cu (0.02 vol.% loading)-nanofluids, respectively, as a function of temperature. It is apparent that with increasing temperature up to ~ 48 °C studied here the thermal conductivity increases monotonically for both the nanofluids at a given volume fraction (low) loading. This happens probably due to the decrease in viscosity of the base fluid with the increase in temperature that leads to increased Brownian motion of the nanoparticles within the base fluid and the consequent higher collision rate of the nanoparticles with the heat source, and so higher collision induced heat transfer. Agglomeration of nanoparticles in a nanofluid is found to be temperature dependent. With increasing temperature, the tendency of nanoparticles for agglomeration decreases (Ref 32). This would have partly caused higher stability and thermal conductivity of nanofluids at higher temperatures. Further, at higher temperature, the surfactant layer capped on the nanoparticles becomes uncapped so that the bare nanoparticle surfaces come in direct contact with the solvent medium and cause increase in the thermal conductivity (Ref 33). A combination of both the surface chemistry of the nanoparticles and Brownian motion causes the higher enhancement in thermal conductivity of nanofluids at higher temperatures. It is interesting to note here that water-based Ag-nanofluid containing only 0.006 vol.% loading exhibits ~ 220% enhancement in thermal conductivity at a temperature of 48 °C with respect to the thermal conductivity of water at room temperature (25 °C). Such a high level of enhancement in thermal conductivity has not been reported earlier in the existing literature and is highly encouraging for the application of this type of nanofluids at high temperature. The outcome of the present study is the development of a highly effective (with respect to both the thermal conductivity and stability) water-based Ag-nanofluid suitable for advanced heat transfer applications, particularly for high-temperature applications. There are reports on the use of

carbon-based nanostructures, viz., carbon nanotubes (CNTs), graphene, to prepare highly stable and effective nanofluids (Ref 34 and 35). However, stability of such kind of nanofluids requires the addition of external surfactant for the functionalization of the carbon nanostructures. In the present study, highly stable and effective nanofluids containing metallic nanoparticles have been produced without use of any external surfactant and hence the present method of synthesis seems to be highly attractive.

Some typical values of thermal conductivity of the present nanofluids at different temperature and volume fraction loading conditions are reported in Table 1, along with those of the conventional fluids. It is obvious from the present study that water-based Ag-nanofluids are far more effective than the conventional heat transfer fluids, particularly at high temperatures (< 48 °C), and have the potential to replace the conventional heat transfer fluids in advanced applications.

4. Conclusion

Chemical reduction method has been used to synthesize silver and copper nanoparticles. The nanoparticles were characterized by UV-Vis, XRD, DLS, SEM, TEM and EDX techniques. The XRD and EDX analysis of the nanoparticles confirmed the presence of elemental silver and copper without any significant impurities. Stable water-based silver nanofluids were obtained without the addition of any dispersant. On the contrary, sedimentation of Cu nanoparticles was observed for higher volume fraction loading of copper particles in ethylene glycol medium. The thermal conductivity of nanofluids has been evaluated as a function of nanoparticles loading using transient hot-wire technique. It has been found that the stabilized silver nanofluid has superior thermal conductivity. But for copper nanofluid, the thermal conductivity increases nonlinearly up to a certain limiting volume fraction, followed by decrease in thermal conductivity at still higher volume fraction, probably due to particles agglomeration effect. Our results unambiguously confirm the important role of agglomeration on the thermal properties of nanofluids. Moreover, markedly higher enhancement of thermal conductivity of nanofluids at high temperature was found. This indicates the likelihood of far better performance of nanofluids at high-

temperature applications as compared to normal room temperature applications.

Acknowledgment

The financial support of the Department of Science and Technology, Government of India, through Grant No. SR/FTP/ETA-118/2011 for executing this project is thankfully acknowledged.

References

1. J.C. Maxwell, *A Treatise on Electricity and Magnetism*, 2nd ed., Oxford University Press, Cambridge, 1904, p 435–441
2. S.U.S. Choi, Nanofluids: From Vision to Reality Through Research, *J. Heat Transf.*, 2009, **131**, p 033106–033109
3. S.A. Kumar, K.S. Meenakshi, B.R.V. Narashimhan, S. Srikanth, and G. Arthanareeswaran, Synthesis and Characterization of Copper Nanofluid by a Novel One-Step Method, *Mater. Chem. Phys.*, 2009, **113**, p 57–62
4. X. Wang, X. Xu, and S.U.S. Choi, Thermal Conductivity of Nanoparticle Fluid Mixture, *J. Thermophys. Heat Transf.*, 1999, **13**, p 474–480
5. S.U.S. Choi, Z.G. Zhang, W. Yu, F.E. Lockwood, and E.A. Grulke, Anomalous Thermal Conductivity Enhancement in Nanotube Suspensions, *Appl. Phys. Lett.*, 2001, **79**, p 2252–2254
6. J.A. Eastman, S.U.S. Choi, S. Li, W. Yu, and L.J. Thompson, Anomalous Increased Effective Thermal Conductivities of Ethylene Glycol-Based Nanofluids Containing Copper Nanoparticles, *Appl. Phys. Lett.*, 2001, **78**, p 718–720
7. A.A. Avramenko, I.V. Shevchuk, A.I. Tyrinov, and D.G. Blinov, Heat Transfer in Stable Film Boiling of a Nanofluid Over a Vertical Surface, *Int. J. Therm. Sci.*, 2015, **92**, p 106–118
8. A. Moghadassi, E. Ghomi, and F. Parvizian, A Numerical Study of Water Based Al_2O_3 and Al_2O_3 -Cu Hybrid Nanofluid Effect on Forced Convective Heat Transfer, *Int. J. Therm. Sci.*, 2015, **92**, p 50–57
9. S.K. Das, N. Putra, P. Thiesen, and W. Roetzel, Temperature Dependence of Thermal Conductivity Enhancement for Nanofluids, *ASME J. Heat Transf.*, 2003, **125**, p 567–574
10. S.M. You, J.H. Kim, and K.H. Kim, Effect of Nanoparticles on Critical Heat flux of Water in Pool Boiling Heat Transfer, *Appl. Phys. Lett.*, 2003, **83**, p 3374–3376
11. A. Ghadimi, R. Saidur, and H.S.C. Metselaar, A Review of Nanofluid Stability Properties and Characterization in Stationary Conditions, *Int. J. Heat Mass Transf.*, 2011, **54**, p 4051–4068
12. N.A. Dhas, C.P. Raj, and A. Gedanken, Synthesis, Characterization and Properties of Metallic Copper Nanoparticles, *Chem. Mater.*, 1998, **10**, p 1446–1452
13. I. Lisiecki, F. Billoudet, and M.P. Pileni, Control of the Shape and the Size of Copper Metallic Particles, *J. Phys. Chem.*, 1996, **100**, p 4160–4166
14. P.J. Jorge, P.S. Isabel, M.L.M. Luis, and M. Paul, Gold Nanorods: Synthesis, Characterization and Applications, *Coord. Chem. Rev.*, 2005, **249**, p 1870–1901
15. X. Zou, E. Ying, and S. Dong, Seed-Mediated Synthesis of Branched Gold Nanoparticles with the Assistance of Citrate and Their Surface Enhanced Raman Scattering Properties, *Nanotechnology*, 2006, **17**, p 4758–4764
16. S. Mehta, S. Kumar, S. Chaudhary, K.K. Bhasin, and M. Gradzielski, Evolution of ZnS Nanoparticles via Facile CTAB Aqueous Micellar Solution Route: A Study on Controlling Parameters, *Nanoscale Res. Lett.*, 2009, **4**, p 17–28
17. V.K. Balakrishnan, X. Han, W.G.W. VanLoon, J.M. Dust, J. Toullec, and E. Bunzel, Acceleration of Nucleophilic Attack on an Organophosphorothioate Neurotoxin, Fenitrothion, by Reactive Counterion Cationic Micelles. Regioselectivity as a Probe of Substrate Orientation Within the Micelle, *Langmuir*, 2004, **20**, p 6586–6593
18. L.P. Wang and G.Y. Hong, A New Preparation of Zinc Sulfide Nanoparticles by Solid-State Method at Low Temperature, *Mater. Res. Bull.*, 2000, **35**, p 695–701
19. E.S. Platonov, I.V. Baranov, S.E. Buravoi, and V.V. Kurepin (E.S. Platonov Ed.), *Thermophysical Measurements: A Manual*, SPbGUN and PT, St. Petersburg, 2010 (in Russian)
20. Y. Xuan and W. Roetzel, Conceptions for Heat Transfer Correlation of Nanofluids, *Int. J. Heat Mass Transf.*, 2000, **43**, p 3701–3707
21. C.J. Yu, A.G. Richter, A. Datta, M.K. Durbin, and P. Dutta, Molecular Layering in a Liquid on a Solid Substrate: An X-Ray Reflectivity Study, *Physica B*, 2000, **283**, p 27–31
22. A.A. Joshi and A. Majumdar, Transient Ballistic and Diffusive Phonon Heat Transport in Thin Films, *J. Appl. Phys.*, 1993, **74**, p 31–39
23. C.W. Shon and M.M. Chen, Microconvective Thermal Conductivity in Disperse Two-Phase Mixture as Observed in a Low Velocity Couette Flow Experiment, *ASME J. Heat Transf.*, 1981, **103**, p 47–51
24. J.C. Maxwell-Garnett, Colours in Metal Glasses and in Metallic Films, *Philos. Trans. R. Soc. Lond. Ser. A*, 1904, **203**, p 385–420
25. G. Paul, S. Sarkar, T. Pal, P.K. Das, and I. Manna, Concentration and Size Dependence of Nano-Silver Dispersed Water Based Nanofluids, *J. Colloid Interface Sci.*, 2012, **371**, p 20–27
26. J. Philip, P.D. Sharma, and B. Raj, Evidence for Enhanced Thermal Conduction Through Percolating Structures in Nanofluids, *Nanotechnology*, 2008, **19**, p 305706
27. M.S. Liu, M.C.C. Lin, C.Y. Tsai, and C.C. Wang, Enhancement of Thermal Conductivity with Cu for Nanofluids Using Chemical Reduction Method, *Int. J. Heat Mass Transf.*, 2006, **49**, p 3028–3033
28. S.K. Das, N. Putra, and W. Roetzel, Pool Boiling Characteristics of Nano-fluids, *Int. J. Heat Mass Transf.*, 2003, **46**, p 851–862
29. K.S. Hong, T.K. Hong, and H.S. Yang, Thermal Conductivity of Fe Nanofluids Depending on the Cluster Size of Nanoparticles, *Appl. Phys. Lett.*, 2006, **88**, p 031901
30. Y. Xuan and Q. Li, Heat Transfer Enhancement of Nanofluids, *Int. J. Heat Fluid Flow*, 2000, **21**, p 58–64
31. J. Philip, P.D. Shima, and B. Raj, Enhancement of Thermal Conductivity in Magnetite Based Nanofluid Due to Chainlike Structures, *Appl. Phys. Lett.*, 2007, **91**, p 203108
32. Y.H. Li, W. Qu, and J.C. Feng, Temperature Dependence of Thermal Conductivity of Nanofluids, *Chin. Phys. Lett.*, 2008, **25**, p 3319–3322
33. H.E. Patel, S.K. Das, T. Sundararajan, A.S. Nair, B. George, and T. Pradeep, Thermal Conductivities of Naked and Monolayer Protected Metal Nanoparticle Based Nanofluids: Manifestation of Anomalous Enhancement and Chemical Effects, *Appl. Phys. Lett.*, 2003, **83**, p 2931–2933
34. S. Mukherjee and S. Paira, Preparation and Stability of Nanofluids: A Review, *IOSR J. Mech. Civ. Eng.*, 2013, **9**, p 63–69
35. R. Taylor, S. Coulombe, T. Otanicar, P. Phelan, A. Gunawan, W. Lv, G. Rosengarten, R. Prasher, and H. Tyagi, Small Particles, Big Impacts: A Review of the Diverse Applications of Nanofluids, *J. Appl. Phys.*, 2013, **113**, p 011301